Hong Kong J Radiol. 2025;28(4):e257-67. Published 10 December 2025 | https://doi.org/10.12809/hkjr2417853

PICTORIAL ESSAY

CME

Exploring the Power of Hybrid Intervention: Utility of an Angiography–Computed Tomography System in Interventional Radiology

CL Wong[1], KKF Fung[2], HY Lo[1], LH Yeung[1], JC Ng[1], KH Lee[1], DHY Cho[1]

[1]Department of Diagnostic and Interventional Radiology, Kwong Wah Hospital, Hong Kong SAR, China
[2]Department of Radiology, Hong Kong Children's Hospital, Hong Kong SAR, China

INTRODUCTION

The use of cross-sectional imaging in interventional radiology (IR) procedures is crucial for accurate target identification, procedure planning, guidance, and immediate therapy response monitoring.

Cone beam computed tomography (CBCT), integrated into angiography systems with flat-panel detectors, has been widely adopted for supplementary cross-sectional imaging during IR procedures, in order to improve procedural precision and safety.

Combined angiography-CT (angio-CT) systems integrate a helical CT scanner and an angiography unit, placed on the same rail with the same patient table. This allows for seamless transition between CT and conventional fluoroscopy/angiography, avoiding the need to move the patient and its attendant risks. Besides achieving a more efficient workflow, it also provides superior image quality in terms of contrast resolution, noise, and artefact reduction, and a larger field of view compared to CBCT.[1] In a study comparing the use of CBCT and angio-CT for transarterial chemoembolisation (TACE), the overall image quality of CT hepatic angiography in angio-CT outperformed that of CBCT in identification of tumour arterial feeders, reduction of streak and respiratory artefacts, resulting in higher overall image quality.[2] Through illustrative cases, we aim to demonstrate the advantages of angio-CT in a wide range of vascular and non-vascular interventions.

ANGIOGRAPHY–COMPUTED TOMOGRAPHY SYSTEM

The angio-CT (Nexaris Angio-CT; Siemens, Tubingen, Germany) which includes a C-arm angiography system and a helical CT scanner installed on the same rail system (Figure 1). During procedures, the patient is positioned with the target organ as close as possible to the CT gantry. While the patient is lying on the IR table for fluoroscopy or angiography, the C-arm can be moved aside to allow the CT gantry to enclose the patient during the procedure, enabling acquisition of three-dimensional

Correspondence: *Dr CL Wong, Department of Diagnostic and Interventional Radiology, Kwong Wah Hospital, Hong Kong SAR, China*
Email: wcl094@ha.org.hk

Submitted: 9 October 2024; Accepted: 24 October 2024.

Contributors: All authors designed the study. CLW and DHYC acquired the data. All authors analysed the data. CLW and KKFF drafted the manuscript, and critically revised the manuscript for important intellectual content. All authors had full access to the data, contributed to the study, approved the final version for publication, and take responsibility for its accuracy and integrity.

Conflicts of Interest: All authors have disclosed no conflicts of interest.

Funding/Support: This study received no specific grant from any funding agency in the public, commercial, or not-for-profit sectors.

Data Availability: All data generated or analysed during the present study are available from the corresponding author on reasonable request.

Ethics Approval: This study was approved by the Clinical Research Ethics Review Board of Hospital Authority, Hong Kong (Ref No.: CIRB-2024-231-3). Informed patient consent was waived by the Board due to retrospective nature of the study.

Figure 1. Setting of angiography–computed tomography. The operator can slide the computed tomography (CT) gantry around the patient table (direction indicated by white arrow) for CT imaging during fluoroscopy/angiography using the control panel next to the patient table (circle).

(3D) image data that can be processed and analysed immediately at the workstation. Immediate fusion of 3D angiography and fluoroscopy allows the operator to navigate to the target during IR procedures such as radioembolisation and TACE, where precision is crucial.

IMAGE ACQUISITION AND INJECTION PROTOCOL CLINICAL APPLICATIONS

Transarterial Chemoembolisation

Improving Visualisation of Small Hepatocellular Carcinoma

Angio-CT with hepatic arteriography outperforms diagnostic CT in terms of hepatocellular carcinoma (HCC) visualisation.[1,3] It can sometimes detect small HCCs that are not conspicuous in magnetic resonance imaging (MRI) or digital subtraction angiography (DSA),[4] as demonstrated in the case below.

A 59-year-old hepatitis B carrier with a history of HCCs at segments 7/8 and 6 (Figure 2 a-c) treated with microwave ablation. During follow-up, alpha-fetoprotein level elevated up to 10 ng/mL. Contrast MRI of the liver showed suspicious multifocal recurrence of HCCs and the patient was referred for TACE. Angio-CT hepatic arteriography demonstrated superior diagnostic power compared to DSA and MRI in detection of subcentimeter HCC with faint arterial enhancement. All lesions demonstrated lipiodol deposition on postprocedural CT, with complete staining, a predictive factor for good therapeutic response to TACE.[3] Alpha-fetoprotein level in follow-up decreased to 7.9 ng/mL (Figure 2).

Improving Visualisation of Extrahepatic Arterial Supply

For HCC cases with extrahepatic supply, studies suggest that angio-CT arteriography offers superior diagnostic capability compared to conventional triphasic CT liver and DSA.[1,4] Its use can increase sensitivity in detecting and confirming parasitic supply, thereby guiding additional treatment strategies.[3,4]

A 77-year-old hepatitis B carrier with a history of left hepatectomy for HCC was later found to have multifocal recurrent HCCs. Multiple TACEs were performed via different branches of the right hepatic artery, but the patient was still found to have persistent right hepatic lobe HCCs on follow-up CT scan (Figure 3).

Enhancing Treatment Efficacy of Drug-Eluting Bead Transarterial Chemoembolisation

In drug-eluting bead (DEB)-TACE, angio-CT offers additional benefits beyond its higher sensitivity for detecting viable tumour components and feeding arteries. Unlike conventional TACE using lipiodol, DEB-TACE does not produce lipiodol staining to assess immediate treatment response. Therefore, an immediate postprocedural angio-CT with intra-arterial contrast injection can help identify residual arterial enhancement and guide further management, such as the need for additional drug administration.

A 64-year-old patient had a large right hepatic lobe HCC. The lesion was too large for resection or ablation. Hence, he underwent several episodes of TACE. However, the patient had poor response with suboptimal tumour lipiodol staining and rapid lipiodol washout, and was referred for DEB-TACE. Right hepatic artery DSA showed three suspicious arterial feeders, which were selectively cannulated with a microcatheter (2.8-Fr Meri Maestro Swanneck microcatheter; Merit Medical Systems, Inc, South Jordan [UT], United States). This case demonstrated the ability of precise identification of feeding arteries in DEB-TACE using angio-CT, particularly for equivocal or indeterminate feeders in DSA and preprocedural CT. It also enabled assessment of immediate treatment response and detection of residual lesions (Figure 4).

Tumour Ablation

Improving Target Visualisation

Identifying target hepatic tumours with ultrasound for

Figure 2. A 59-year-old patient. (a-c) Magnetic resonance imaging (MRI) of the liver with gadoxetic acid contrast in the arterial phase shows suspicious multifocal subcentimeter recurrent hepatocellular carcinoma in segments 6, 7 and 8 (arrows). The arrow in (c) indicates a faint arterial enhancing focus at segment 6 near the liver edge. (d) Right hepatic artery digital subtraction angiography shows no tumour blush in the MRI detected lesions. (e-g) Angiography–computed tomography (Angio-CT) with intra-arterial contrast injection into the right hepatic artery shows multiple arterial-phase enhancing lesions corresponding to the MRI-detected tumours as seen in (a) to (c) [arrowheads]. Chemoembolisation was performed. (h-j) Immediate post–transarterial chemoembolisation plain CT on the angio-CT system shows lipiodol uptake in target lesions (dashed arrows). All lesions demonstrated lipiodol deposition on the postprocedural scan, with complete staining seen in (i) and (j).

ablation can be difficult due to cirrhotic liver or prior treatment changes. Contrast CT significantly helps with lesion identification and ablation probe placement. Some operators also perform intraprocedural angio-CT with intra-arterial injection for tumour identification and ablation margin monitoring,[1,4] improving the precision of ablation and treatment response monitoring.

Increasing Ease for Artificial Ascites Creation

For creation of artificial ascites, an angio-catheter is first inserted into the peritoneal space under ultrasound guidance, followed by a guidewire, then exchanged to a catheter for dextrose infusion. Using angio-CT, operators can safely manipulate the guidewire and exchange to the catheter under real-time fluoroscopy, confirm catheter position on CT, and proceed to image-guided ablation. All steps involving different imaging modalities can be performed on the same table without moving the patient.

Radiofrequency Ablation of Liver Metastases

An 85-year-old patient with a history of colonic cancer and prior liver metastases treated with ablations. Follow-up CT showed several new liver metastases, and the patient was referred for image-guided radiofrequency ablation. On-table ultrasound identified several nodules in the right hepatic lobe, but it was difficult to distinguish

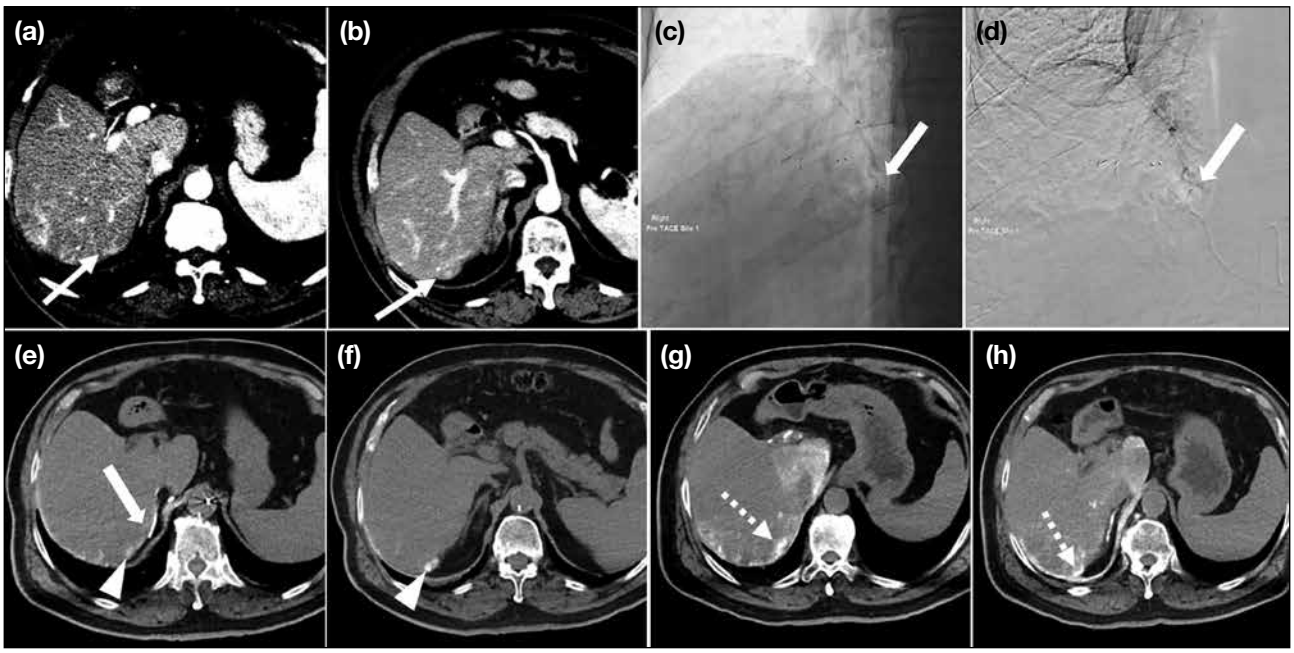

Figure 3. A 77-year-old patient. (a, b) Contrast computed tomography (CT) of the liver in late arterial phase shows several faint enhancing lesions in the right hepatic lobe suspicious for recurrent hepatocellular carcinoma (arrows). Contrast CT was unable to identify the extrahepatic feeding artery. Given the location of these lesions, the right inferior phrenic artery was thought to be one of the common extrahepatic supplies. (c, d) The right inferior phrenic artery was cannulated with a 1.7-Fr microcatheter (arrows) [Merit Pursue; Merit Medical Systems, Warrington (PA), United States]. (d) Digital subtraction angiography shows no sizable tumour blush. (e, f) Angiography–computed tomography (angio-CT) with intra-arterial injection of the right inferior phrenic artery confirmed it supplying the right hepatic lesions (arrowheads). A chemotherapeutic mixture was administered via microcatheter (arrow in [e]). (g, h) Postprocedural plain CT on the angio-CT system performed after several additional sessions of transarterial chemoembolisation, shows dense lipiodol uptake (dashed arrows) and a reduction in lesion size, as seen in (h).

them from prior ablation zones. Triphasic angio-CT liver showed several liver metastatic lesions (Figure 5).

Acute Haemorrhage Embolisation

Improving Detection of Bleeding Source

In cases of acute bleeding, angio-CT angiogram can detect bleeding sources too small or slow to be identified on CT with intravenous contrast.[1] With 3D reformatting, the precise location of the bleeder can be accurately determined.

Quicker Cessation of Bleeder

Unstable patients with active bleeding can be transferred directly to angio-CT for urgent CT, followed by immediate embolisation on the same table. This eliminates the need to move patients between the diagnostic CT and IR suites, allowing quicker haemorrhage control and improved outcomes.

Embolisation of Haemorrhagic Renal Tumour

A 70-year-old patient was incidentally found to have an enhancing soft tissue mass at the lower pole of left kidney. Ultrasound-guided biopsy was performed, but the patient developed left flank pain with a haemoglobin drop from 14.1 g/dL to 11.6 g/dL on day 1 post-biopsy. Urgent CT of the kidney found intratumoural haemorrhage and trace left haemoretroperitoneum. Post-embolisation haemoglobin level remained stable, with post-embolisation day 5 follow-up CT showing no progression or active bleeding. The patient was later discharged (Figure 6).

Endoleak Detection and Management

Diagnosis for Endoleak

Angio-CT combines the benefits of DSA and CT by integrating real-time flow dynamics with detailed cross-sectional anatomy. This allows comprehensive and accurate evaluation of the type and site of endoleak, as demonstrated in the following case.

A 76-year-old male patient with infrarenal abdominal aortic aneurysm and left common and internal iliac artery aneurysms was managed with endovascular aneurysm repair. A diagnostic aortogram was performed 1 year after endovascular aneurysm repair to clarify the type and site of endoleak. 5-Fr Multipurpose catheter (Merit

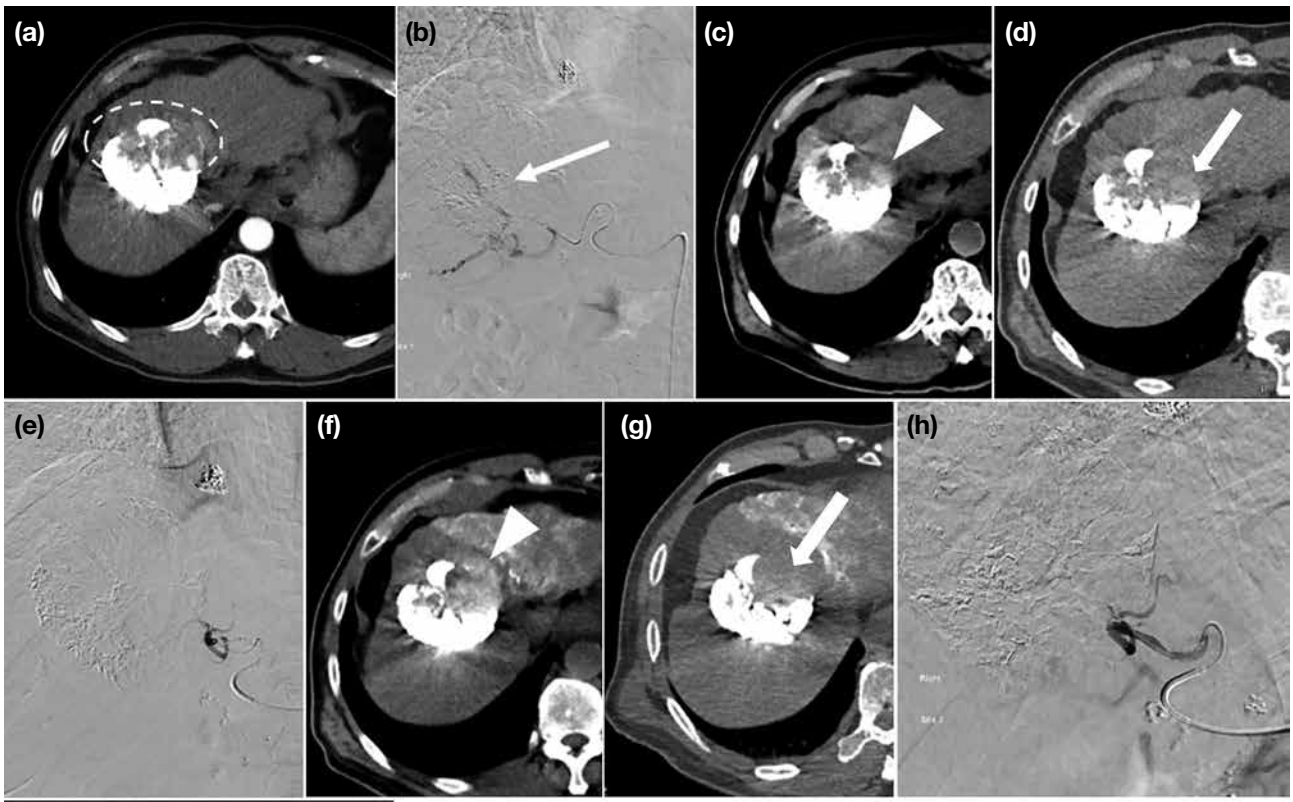

Figure 4. A 64-year-old patient. (a) Preprocedural contrast computed tomography of the liver in late arterial phase, showing poor lipiodol staining at the anterior aspect of the lesion with a viable arterial enhancing component (dashed circle). (b) Target site 1 cannulated with microcatheter. Digital subtraction angiography (DSA) showed tumour blush (arrow). (c) The arterial component was confirmed with intra-arterial injection using angiography–computed tomography (angio-CT), showing arterial blush (arrowhead). Drug-eluting beads loaded with chemomixture were administered. (d) Immediate post–drug-eluting bead transarterial chemoembolisation (DEB-TACE) angio-CT with intra-arterial injection at the feeder showing reduction in the enhancing component (arrow). (e) DSA of Target site 2 shows no sizable tumour blush. (f) However, angio-CT with an intra-arterial injection shows arterially enhancing viable component (arrowhead). Drug-eluting beads loaded with chemomixture were administered. (g) Immediate post–DEB-TACE angio-CT with intra-arterial injection at feeder shows significant reduction in arterial enhancing component (arrow). (h, i) DSA of Target site 3 shows no sizable tumour blush, in concordance with intra-arterial injection angio-CT showing no arterial enhancing viable component. No drug was administered at this site.

Medical, South Jordan [UT], United States) was then navigated to the left iliac limb and superior mesenteric artery, with angio-CT angiogram performed to exclude other endoleak sites. The patient was managed with extension of the right iliac limb endograft (Figure 7).

Embolisation of Endoleak

Angio-CT is useful for endoleak treatment. A CT aortogram with intra-arterial injection enables precise localisation of the endoleak, followed by targeting under combined CT and fluoroscopic guidance, and embolisation under real-time fluoroscopy. Final placement of embolic material and any immediate complications can be verified with angio-CT. The system allows the entire multimodality process to be performed on the same table.

An 86-year-old male patient with an infrarenal abdominal aortic aneurysm, bilateral common iliac artery and IIA aneurysms was treated with endovascular aneurysm repair, right IIA coil embolisation and left iliac bifurcation device. The endoleak was targeted for balloon-assisted percutaneous transluminal glue embolisation in the same session. With angio-CT enabling seamless, efficient transition between CT angiogram and fluoroscopy, the operator safely targeted the endoleak site for embolisation without injuring adjacent organs or damaging the stent (Figure 8).

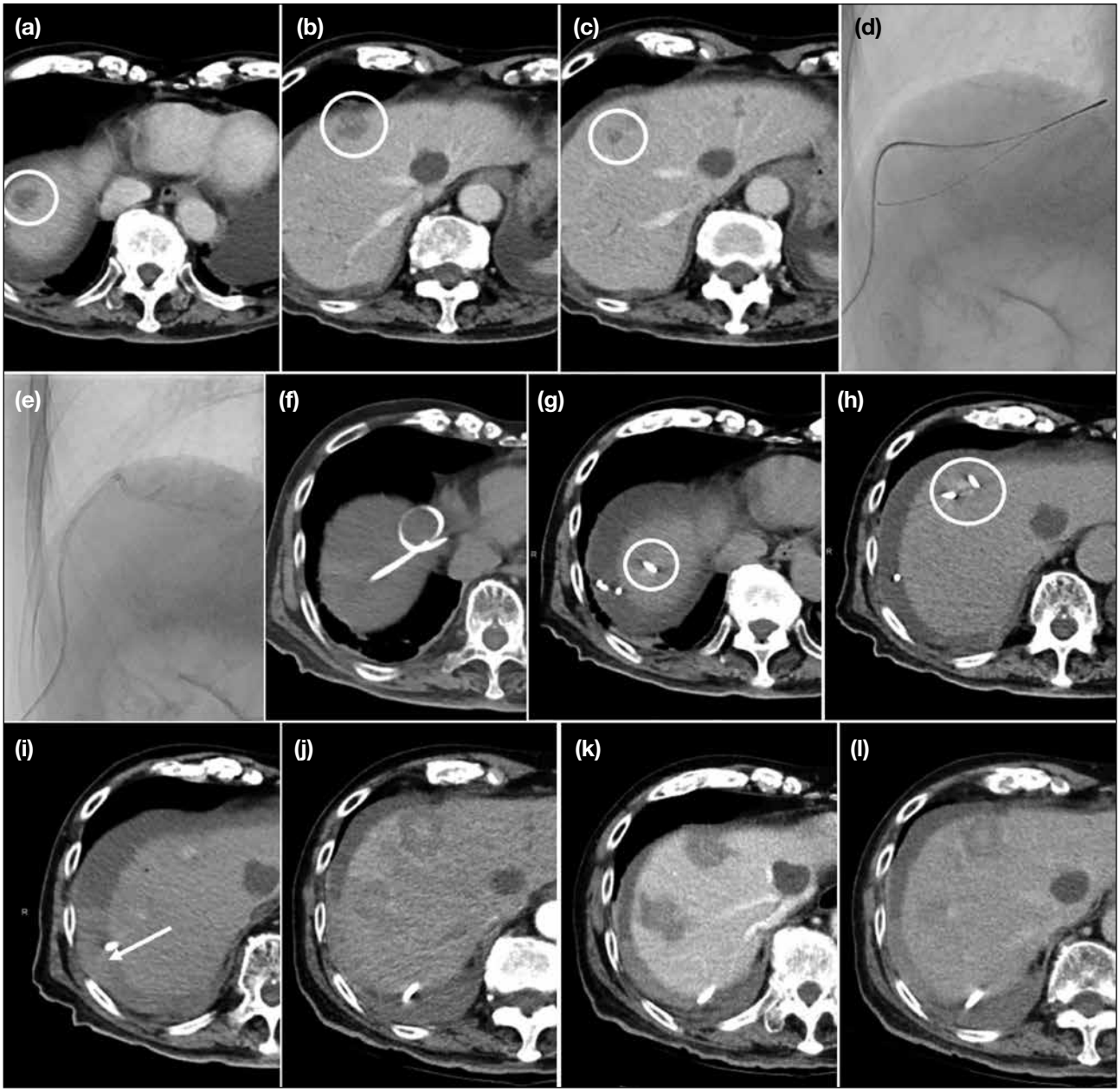

Figure 5. (a-c) An 85-year-old male patient. Three hypoenhancing nodules in segments 8 and 4a (circles), suggestive of liver metastases. (d-f) For creation of artificial ascites, a 16-gauge angio-catheter (Becton Dickson, Franklin Lakes [NJ], US) was used to target the perihepatic space under ultrasound guidance, which was then exchanged to a 6-Fr catheter (Boston Scientific, Marlborough [MA], US) over a 0.035-inch guidewire (Terumo, Tokyo, Japan) under fluoroscopy. The catheter tip was confirmed with angiography–computed tomography (angio-CT), followed by infusion of 5% dextrose solution. (g, h) Each lesion was targeted with an ablation antenna under ultrasound and computed tomography (CT) guidance (antenna tips indicated by circles), with a 12-minute ablative cycle performed. (i) Postprocedural CT showing a hyperdense layer (arrow) in the artificial ascites and noted blood-stained fluid in drain. (j-l) Immediate multiphasic images were acquired by angio-CT, showing no evidence of active bleeding or pseudoaneurysm. The patient's vital signs were stable and he was sent back to the ward for close observation.

Other Cross-Modalities Applications

Percutaneous Embolisation of Pulmonary Vein Pseudoaneurysm

The angio-CT system is valuable in complex IR cases requiring precise target localisation with CT and real-time fluoroscopic guidance, as illustrated in the following case. An 88-year-old patient with multiple co-morbidities and a history of Stanford type A aortic dissection managed conservatively was admitted with haemoptysis of 50 to 100 mL/day. Haemoglobin level dropped from 10.8 g/dL to 7.7 g/dL despite on transamin and repeated blood transfusions. He required oxygen

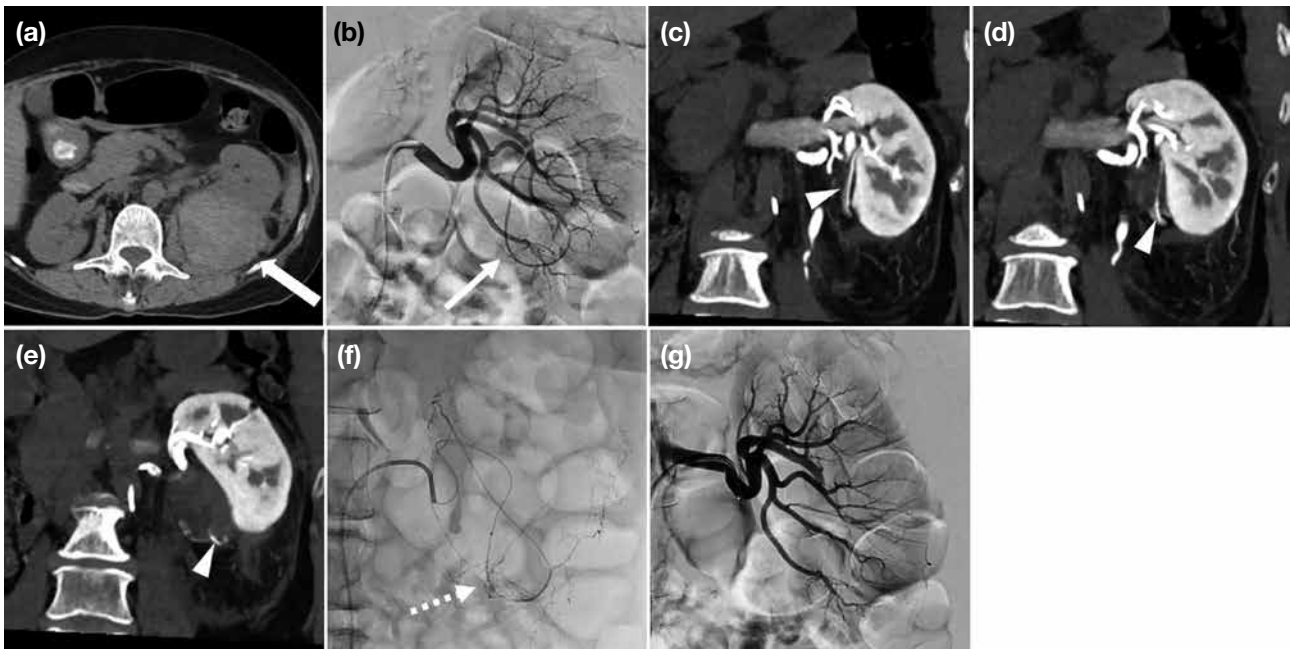

Figure 6. (a) A 70-year-old patient. Pre-contrast computed tomography (CT) of the kidneys shows a left renal lower pole mass with internal hyperdensities (arrow), suggesting intratumoural haemorrhage. Arterial phase CT shows no pseudoaneurysm or active contrast extravasation. (b) The left main renal artery was cannulated with a catheter (5-Fr C1 catheter; Cordis, Miami Lakes [FL], US) and digital subtraction angiography (DSA) performed, showing a long curved tortuous inferior segmental artery to the left lower pole (arrow), with dysplastic distal branches. (c-e) With angiography–computed tomography, this was confirmed to be the feeding artery (arrowheads) to the haemorrhagic renal lesion, without pseudoaneurysm or active contrast extravasation. (f) The feeder was selectively cannulated with a 2.4-Fr microcatheter (Maestro; Merit Medical Systems, Warrington [PA], US) with DSA confirming its supply to the renal lesion (dashed arrow). Embolisation was performed with Embospheres 500-700 μm (Merit, Warrington [PA], US) until stasis was achieved. (g) Check of left renal angiogram showing successful occlusion of the bleeding artery.

support at 2 L/min via mask. An urgent CT aortogram was performed, and the patient was referred for angiogram for lesion characterisation and subsequent management. His condition improved, with haemoptysis level reduced to 10 mL/day. Haemoglobin level remained stable at 7 to 8 g/dL and oxygen support was weaned off (Figure 9).

This case demonstrates successful lesion targeting using a percutaneous approach, where reliance on either fluoroscopy or intermittent CT alone poses a high risk of injury to vital internal organs. With the advantage of angio-CT allowing seamless transition between CT and fluoroscopy, the operator safely punctured the target without harming surrounding organs, followed by embolisation under real-time fluoroscopy.

Adrenal Venous Sampling

Recognition and cannulation of the right adrenal vein is one of the most challenging aspects of adrenal venous sampling (AVS). Common issues include catheter dislodgement, incorrect or deep cannulation, or anatomical variants like an accessory hepatic vein that may dilute cortisol. In such cases, CT during AVS can help delineate anatomy and confirm catheter position.[5] Compared to CBCT, CT offers superior image quality and faster acquisition, reducing the risk of catheter dislodgement. A case illustration is presented below.

A 42-year-old female patient with primary hyperaldosteronism and hypertension previously failed AVS, as the right adrenal venous sample lacked sufficient cortisol to meet the required selectivity index, despite venography showing a typical spidery configuration on retrospective review. The cause of failure was indeterminate and she was referred for a second AVS. Angio-CT right venogram was performed before and just after right sampling to: (1) ensure correct cannulation of the right adrenal vein; (2) ensure the catheter remained in situ during sampling; and (3) exclude anatomical variants such as an accessory hepatic vein. Post-sampling angio-CT confirmed catheter position. Sampling of right adrenal veins was successful reaching a selectivity index of 15. The patient was diagnosed with a left-sided aldosterone-secreting tumour and is pending surgery (Figure 10).

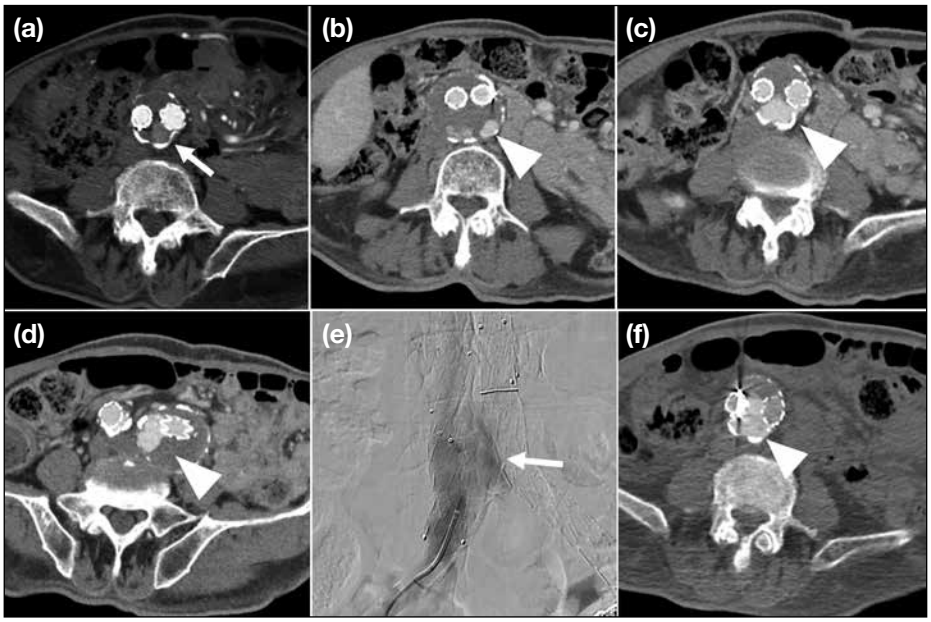

Figure 7. A 76-year-old male patient. (a) Initial computed tomography aortogram shows endoleak within posterior aspect of the distal aortic aneurysmal sac (arrow). It was originally thought to be a type II endoleak from the median sacral artery. (b-d) Upon follow-up computed tomography aortography increasing diameters of abdominal aortic aneurysm and left common iliac artery aneurysm were noted, with increased endoleak within the aortic aneurysmal sacs (arrowheads). (e) An aortogram with intra-arterial injection in the right iliac limb. There was abnormal contrast leakage near the distal abdominal aortic aneurysm sac and the right common iliac artery aneurysmal sac (arrow). (f) Angiography–computed tomography with intra-arterial contrast injection via the right iliac limb shows an endoleak originating from the right iliac endograft, consistent with a type IB endoleak (arrowhead).

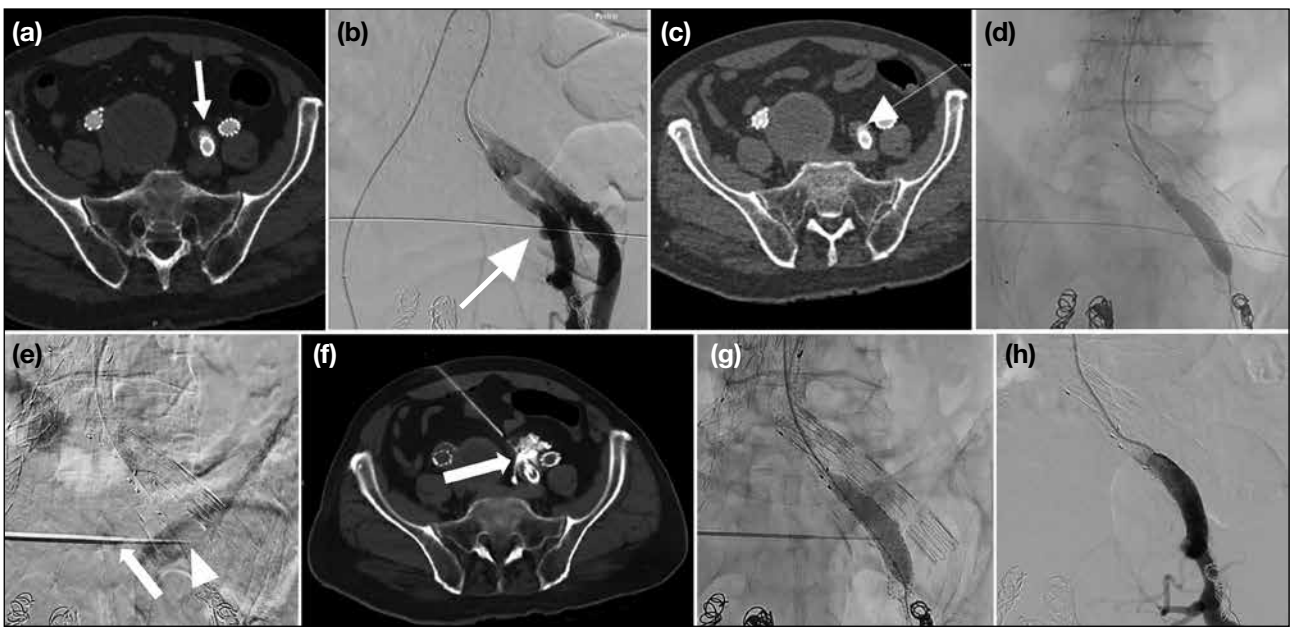

Figure 8. An 86-year-old male patient. (a) Initial computed tomography aortogram showing increase in size of abdominal aortic aneurysm sac and left IIA sac, with only mild endoleak suspected near the left internal iliac limb (arrow). (b, c) Aortogram and angiography–computed tomography (angio-CT) respectively, with intra-arterial injection at common iliac limb at left iliac bifurcation device, confirming left internal iliac limb endoleak (arrows). (d) Successful cannulation of the left internal iliac artery limb and deployment of a 10 mm × 40 mm balloon (Mustang, Boston [MA], US) at the site of the endoleak with position confirmed with angio-CT. (e) Under combined computed tomography (CT) and fluoroscopic guidance, a 17-gauge needle (arrow) [Gangi-SoftGuard; Apriomed, Uppsala, Sweden] was advanced towards the site of the endoleak in the left internal iliac artery (IIA) via the right anterior abdominal wall, through which a 20-gauge Chiba needle (Cook Medical, Bloomington [IN], US) [arrowhead] was introduced to puncture the left IIA endoleak site. (f) The position of the Chiba needle (arrow) was confirmed by CT and fluoroscopy with contrast injection. (g) A 10 mm × 40 mm 135-cm balloon (Mustang; Boston Scientific, Marlborough [MA], US) was inflated to occlude the endoleak site whilst total of 1.5 mL of hutyl cyanoacrylate glue (50% dilution with lipiodol) was injected under real time fluoroscopy. The balloon was then withdrawn. (h) Post-embolisation angiogram shows satisfactory obliteration of the left internal iliac limb endoleak.

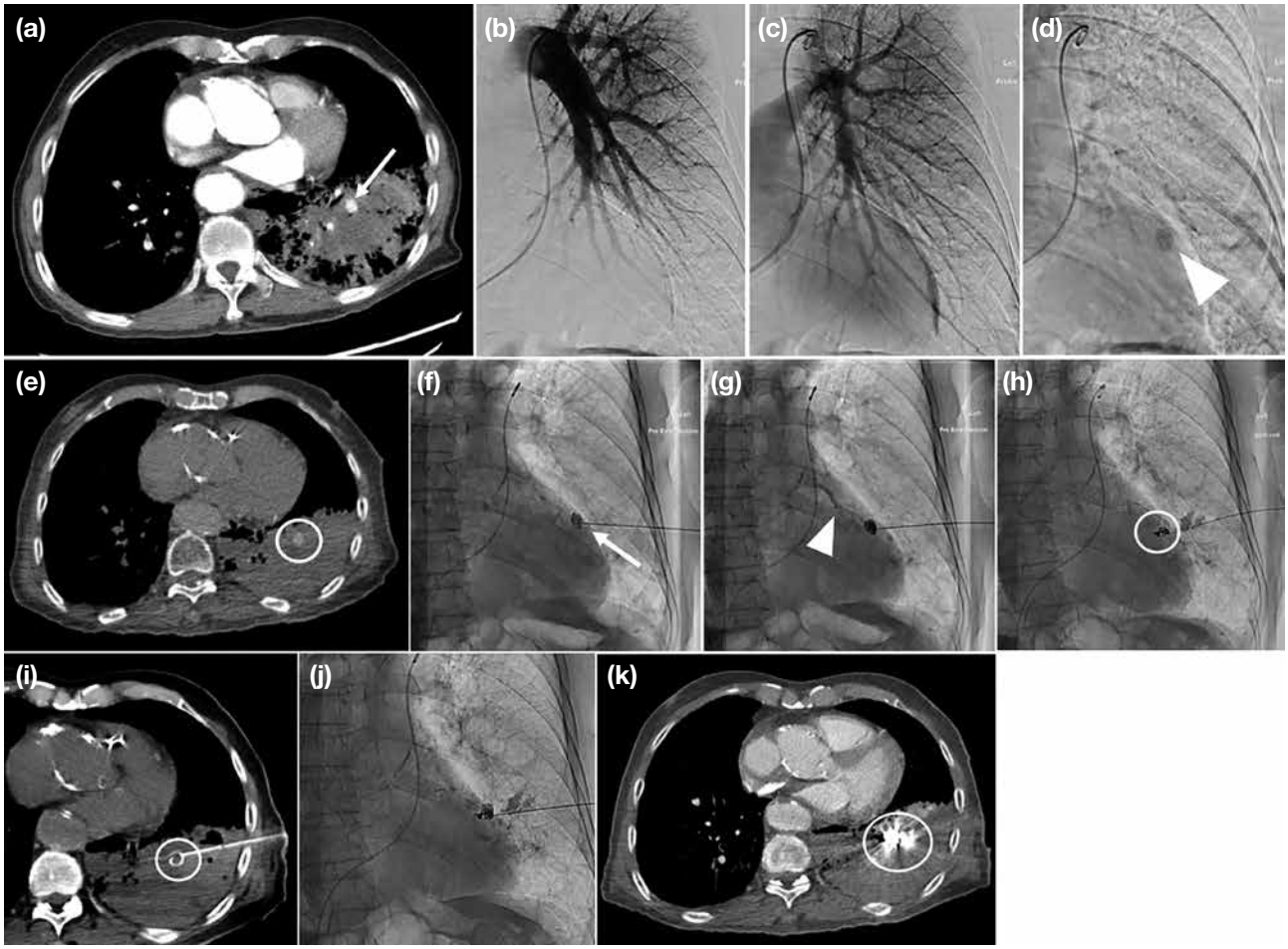

Figure 9. (a) An 88-year-old patient. Urgent computed tomography aortogram showing pulmonary consolidation and haemorrhage in the left lower lobe, with a 0.9-cm enhancing lesion within the consolidation (arrow). It is closely abutting the left inferior pulmonary vein, raising suspicion of a pulmonary venous pseudoaneurysm. Known Stanford type A aortic dissection was static with no mediastinal haematoma. (b, c) Left pulmonary angiogram shows no corresponding lesion in the left lower lobe in pulmonary arterial and parenchymal phases. (d, e) An enhancing nodule in the left lower lobe appeared after pulmonary arterial and parenchymal phases (arrowhead in [d]), consistent with the computed tomography (CT) findings that it originated from the left inferior pulmonary vein rather than pulmonary artery. The location was confirmed in angiography–computed tomography (circle in [e]) for embolisation planning. (f, g) Under combined fluoroscopic and CT guidance, a 20-gauge Chiba needle (Cook Medical, Bloomington [IN], US) was used to percutaneously access the pseudoaneurysm sac. Under fluoroscopy, contrast injection confirmed needle positioning with opacification of the pseudoaneurysm sac (arrow in [f]) and the outflowing pulmonary vein (arrowhead in [g]). (h, i) Two 4 mm × 10 cm embolisation coils (Concerto; Medtronic, Minneapolis [MN], US) [circle in (h)] were successfully deployed under fluoroscopy, with coil position confirmed with CT (circle in [i]). (j) Further attempt coiling of aneurysm was not successful. 0.6 mL of hutyl cyanoacrylate glue (50% dilution with lipiodol) was injected under fluoroscopy for complete sac embolisation. (k) Postprocedural CT shows complete obliteration of the pseudoaneurysm by glue and coils without residual contrast opacification (circle).

Details of the contrast injection and image acquisition protocols for commonly performed vascular procedures requiring CT acquisition with our angio-CT system are provided in the Table.

DISCUSSION

The above cases highlight the applications and advantages of using the angio-CT system in various IR procedures. Compared to CBCT previously used in our unit, the image quality of CT hepatic angiogram in angio-CT surpasses CBCT in visualisation of tumour, identification of tumour arterial feeders, reduction of streaking artefacts, wider field of view including the whole liver, fewer respiratory motion artefacts, and higher overall subjective image quality[2] (Figure 11). It also allows immediate postprocedural imaging to assess treatment response, such as immediate lipiodol uptake and presence of residual lesions, which are limited by streaking and respiratory artefacts in CBCT.

For angio-CT hepatic arteriogram, a smaller amount of contrast can be used for direct hepatic artery injection

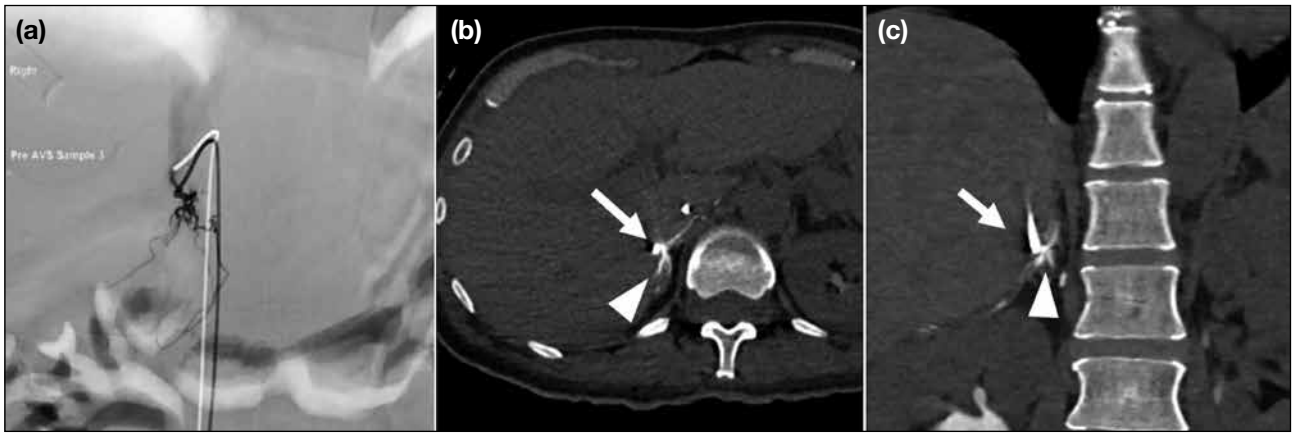

Figure 10. (a) A 42-year-old female patient. During second trial of adrenal venous sampling (AVS), the right adrenal vein was cannulated with a catheter (Yashiro; Terumo, Tokyo, Japan). Right adrenal venogram shows the spidery configuration of the right adrenal vein, similar to previous AVS. (b, c) Angiography–computed tomography right adrenal venogram before sampling shows catheter tip (arrows) was within the right adrenal vein, with contrast opacification of the right adrenal gland (arrowheads). There was no accessory vein draining to the right adrenal vein. The injection protocol via the 5-Fr Yashiro catheter was: 6 mL undiluted contrast at 1 mL/sec, with computed tomography acquisition at 4 seconds after start of contrast injection.

Table. Contrast injection and image acquisition protocol in our unit for some common interventional radiology procedures that might require the use of angiography–computed tomography.

Procedure	Catheter size and site of contrast injection	Contrast medium (iohexol 350 mg) injection protocol
TACE	4- or 5-Fr catheter positioned at common or proper hepatic artery	22-mL undiluted contrast in 2 mL/s, followed by 10 mL of normal saline in 0.5 mL/s - Early arterial phase CT acquisition at 8 s after start of contrast injection - Late arterial phase CT acquisition at 18 s after start of contrast injection
	2.0- or 2.5-Fr microcatheter positioned at right/left hepatic arteries or segmental hepatic branches	9-mL undiluted contrast in 0.5-1 mL/s, followed by 10 mL of normal saline in 0.5 mL/s - Early arterial phase CT acquisition at 6 s after start of contrast injection - Late arterial phase CT acquisition at 17 s after start of contrast injection
Endovascular aneurysm repair or endoleak management	4- or 5-Fr pigtail catheter positioned at abdominal aorta	30-mL diluted contrast (contrast-to–normal saline ratio = 1:5) in 7 mL/s - Aortogram acquired at 6 s after start of contrast injection

Abbreviations: CT = computed tomography; TACE = transarterial chemoembolisation.

compared to systemic intravenous injection.[4,5] In DEB-TACE, multiple contrast injections are typically required to verify target lesions. Therefore, using angio-CT may help reducing fluid overload and contrast load, which is beneficial to patients with liver cirrhosis with pre-existing fluid status disturbances.

In suspected complications during or immediately after IR, angio-CT can be promptly performed with multiphasic studies to detect bleeding, without transferring the patient to diagnostic CT. This allows immediate diagnosis and treatment, such as urgent embolisation.

Apart from the above examples, angio-CT can improve procedural outcomes in the following scenarios.

A common application is combined TACE and ablation for liver cancers, where TACE is first performed first to devascularise and stain the tumour, followed by ablation in the same session. The ablation margin can be monitored during and after with intra-arterial contrast injection, improving margin visualisation.

In hypervascular soft tissue or bone tumours, such as renal cell or thyroid carcinoma bone metastases, embolisation can be done first under angiography to reduce its vascularity, followed by CT-guided ablation in the same session. This reduces haemorrhagic risks, especially in hypervascular tumours.[5,7]

In emergencies requiring urgent embolisation, such

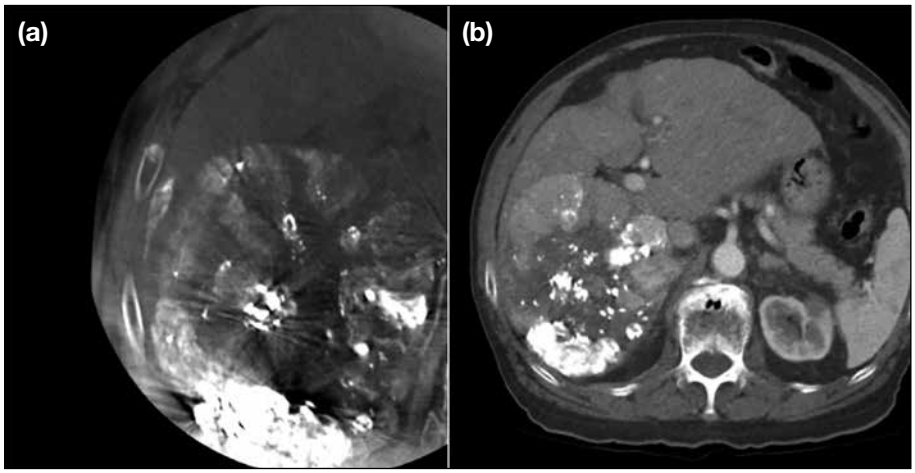

Figure 11. (a) Cone beam computed tomography (CBCT) of the liver in a patient with large right hepatic tumour after transarterial chemoembolisation (TACE). There are marked streaking artifacts obscuring assessment of the structures. (b) Angiography–computed tomography after TACE of the same patient. Compared to CBCT, it shows significant improvement of image quality with less streaking artifacts, fewer respiratory motion artifacts and wider field of view.

as trauma or ruptured HCC, the patient can be directly transferred to angio-CT for urgent CT angiogram and embolisation. After reviewing images on the angio-CT workstation, the operator can proceed immediately without transferring the patient from diagnostic CT to IR suite. This is crucial when the patient is haemodynamically unstable and also shortens scan-to-needle time, potentially improving outcomes.

A major drawback of angio-CT is cost and space. Depending on vendor and performance, angio-CT is approximately 1.5 to 2 times more expensive than flat panel CBCT.[8] It also requires more space compared with C-arm CBCT, possibly needing re-design of the IR suite.

Radiation dose between angio-CT and CBCT remains debated. A study on CT-guided lung biopsy showed angio-CT delivered 1.2 to 1.7 times higher effective dose than CBCT (mean: 15.77 mSv vs. 10.68 mSv).[9] However, another study during TACE showed angio-CT had 2.5 times lower effective dose than CBCT (median: 15.4 vs. 39.2 mSv).[10] Dose indices differ: angio-CT uses dose-length product while CBCT uses dose-area product. As these comparisons were based on estimated effective doses using region-specific conversion factors and phantom calculations, uncertainties must be considered when interpreting dosage results.

The integration of angiography unit and dedicated CT scanner into a hybrid angio-CT system is a revolutionary technology for IR. By enabling detailed anatomical characterisation and visualisation of critical structures, angio-CT is a valuable tool to enhance the patient outcome and reduce procedural risks in complex interventional procedures.

REFERENCES

1. Taiji R, Lin EY, Lin YM, Yevich S, Avritscher R, Sheth RA, et al. Combined angio-CT systems: a roadmap tool for precision therapy in interventional oncology. Radiol Imaging Cancer. 2021;3:e210039.
2. Lin EY, Jones AK, Chintalapani G, Jeng ZS, Ensor J, Odisio BC. Comparative analysis of intra-arterial cone-beam versus conventional computed tomography during hepatic arteriography for transarterial chemoembolization planning. Cardiovasc Intervent Radiol. 2019;42:591-600.
3. Wang H, Han Y, Chen G, Jin L. Imaging biomarkers on angio-CT for predicting the efficacy of transarterial chemoembolization in hepatocellular carcinoma. Quant Imaging Med Surg. 2023;13:4077-88.
4. van Tilborg AA, Scheffer HJ, Nielsen K, van Waesberghe JH, Comans EF, van Kuijk C, et al. Transcatheter CT arterial portography and CT hepatic arteriography for liver tumor visualization during percutaneous ablation. J Vasc Interv Radiol. 2014;25:1101-11.e4.
5. Kobayashi K, Ozkan E, Tam A, Ensor J, Wallace MJ, Gupta S. Preoperative embolization of spinal tumors: variables affecting intraoperative blood loss after embolization. Acta Radiol. 2012;53:935-42.
6. Puijk RS, Nieuwenhuizen S, van den Bemd BA, Ruarus AH, Geboers B, Vroomen LG, et al. Transcatheter CT hepatic arteriography compared with conventional CT fluoroscopy guidance in percutaneous thermal ablation to treat colorectal liver metastases: a single-center comparative analysis of 2 historical cohorts. J Vasc Interv Radiol. 2020;31:1772-83.
7. Owen RJ. Embolization of musculoskeletal bone tumors. Semin Intervent Radiol. 2010;27:111-23.
8. Tanaka T, Arai Y, Inaba Y, Inoue M, Nishiofuku H, Anai H, et al. Current role of hybrid CT/angiography system compared with C-arm cone beam CT for interventional oncology. Br J Radiol. 2014;87:20140126.
9. Strocchi S, Colli V, Conte L. Multidetector CT fluoroscopy and cone-beam CT-guided percutaneous transthoracic biopsy: comparison based on patient doses. Radiat Prot Dosimetry. 2012;151:162-5.
10. Piron L, Le Roy J, Cassinotto C, Delicque J, Belgour A, Allimant C, et al. Radiation exposure during transarterial chemoembolization: angio-CT versus cone-beam CT. Cardiovasc Intervent Radiol. 2019;42:1609-18.